



UNIVERSITY OF LEEDS

This is a repository copy of *Achieving Driving Comfort of AVs by Combined Longitudinal and Lateral Motion Control*.

White Rose Research Online URL for this paper:
<http://eprints.whiterose.ac.uk/148723/>

Version: Accepted Version

Proceedings Paper:

Wei, C orcid.org/0000-0002-4565-509X, Romano, R orcid.org/0000-0002-2132-4077, Merat, N orcid.org/0000-0002-2132-4077 et al. (4 more authors) (2020) Achieving Driving Comfort of AVs by Combined Longitudinal and Lateral Motion Control. In: Advances in Dynamics of Vehicles on Roads and Tracks. IAVSD 2019. Lecture Notes in Mechanical Engineering. 26th IAVSD International Symposium on Dynamics of Vehicles on Roads and Tracks, 12-16 Aug 2019, Gothenburg, Sweden. Springer , pp. 1107-1113. ISBN 978-3-030-38076-2

https://doi.org/10.1007/978-3-030-38077-9_129

© Springer Nature Switzerland AG 2020. Uploaded in accordance with the publisher's self-archiving policy.

Reuse

Items deposited in White Rose Research Online are protected by copyright, with all rights reserved unless indicated otherwise. They may be downloaded and/or printed for private study, or other acts as permitted by national copyright laws. The publisher or other rights holders may allow further reproduction and re-use of the full text version. This is indicated by the licence information on the White Rose Research Online record for the item.

Takedown

If you consider content in White Rose Research Online to be in breach of UK law, please notify us by emailing eprints@whiterose.ac.uk including the URL of the record and the reason for the withdrawal request.



eprints@whiterose.ac.uk
<https://eprints.whiterose.ac.uk/>

Achieving Driving Comfort of AVs by Combined Longitudinal and Lateral Motion Control

Chongfeng Wei*, Richard Romano, Natasha Merat, Foroogh Hajiseyedjavadi, Albert Solernou, Evangelos Paschalidis, Erwin R. Boer

Institution for Transport Studies, University of Leeds, Leeds LS2 9JT, UK

*Email: c.wei2@leeds.ac.uk

Abstract. As automated vehicles (AVs) are moving closer to practical reality, one of the problems that needs to be resolved is how to achieve an acceptable and natural risk management behaviour for the on-board users. Cautious automated driving behaviour is normally demonstrated during the AV testing, by which the safety issue between the AV and other road users or other static risk elements can be guaranteed. However, excessive cautiousness of the AVs may lead to traffic congestion and strange behaviour that will not be accepted by drivers and other road users. Human-like automated driving, as an emerging technique, has been concentrated on mimicking a human driver's behaviour in order that the behaviour of the AVs can provide an acceptable behaviour for both the drivers (and passengers) and the other road users. The human drivers' behaviour was obtained through simulator based driving and this study developed a nonlinear model predictive control to optimise risk management behaviour of AVs by taking into account human-driven vehicles' behaviour, in both longitudinal and lateral directions.

Keywords: Automated Vehicle, Vehicle Motion Control, Human-Mimicked Control, Human-like Control.

1 Introduction

Motion planning and trajectory following are important components for the AV motion control. For the collision avoidance scenario, the path is normally planned to avoid the obstacles, and then make the AV exactly follow the designed path [1,2]. However, it may lead to some uncomfortable human experiences in terms of the high acceleration and jerk. Although the AV can follow the desired lateral offset and heading angle of the vehicle, exact following may not be needed. Therefore, determination of a safety corridor is more practical than merely planning a path. The corridor can be determined by allowing the vehicle to stay away from the risk elements while simultaneously providing the drivers a sense of security and comfort. Comfortable trajectory can be obtained when we optimize the vehicle's motion during AV control within the safe corridor. In this way, both comfortability and sense of the security can be achieved.

However, corridor planning does not mean neglect of the desired path, as we don't expect the vehicle to move far away laterally from the desired path during pursuing

comfortability, and higher speed error relative to the driver's desired speed is also not expected. To this end, we investigate the drivers' behaviour while risk elements are present alongside and within the driver's lane such as parked cars and designed the motion controller to mimic drivers' behaviour.

2 Drivers' behavior

We explore driver behavior on simulated roads with different elements along side the road such as hedges and curbs as well as on the road such as parked cars or road works [3].

2.1 Longitudinal desired speed

The observed speed and lateral position from the simulation experiment with a driver simulator is used to derive the human-like desired speed, speed tolerance and lateral offset tolerance. Table 1 shows the observed median speeds and standard deviations from the experiment for four specific roadway conditions with 44 participants. Each of these conditions was persisted for 250m and the center portion was used to estimate steady state median and STD speed; please refer [3] for our experimental design details.

Table 1. Median speed and standard deviation of speed obtained from driving tests

Environ- ment	Curve	Context	Curve direction	Median Speed (mps)	Standard Deviation of Speed (mps)
'rural'	170	'grass'	'curve-right'	20.3263	2.8062
'rural'	'straight'	'asphalt'	'straight'	25.1421	3.9073
'rural'	'250'	'hedge'	'curve-left'	21.4319	3.1623
'urban'	'straight'	'blockage'	'straight'	19.4599	2.8847

The median observed speed is considered as the desired speed (or reference speed) for the AV motion control. However, the AV does not need to follow the speed exactly. The acceptable speed range around the target we define based on our risk model [4].

2.2 Lateral offset variation

Vehicle lateral offset variation determines the drivers' behavior in controlling the vehicle to steer around the risk elements and increase their sense of security by managing risk [5], i.e. time to lane crossing [4]. For example, static obstacles could be parked cars located at the roadside at the middle of a 250 m long road. This scenario represents the risk level variation from a low-level risk away from the parked car to a higher potential risk close to the parked car. Drivers naturally slow down and swerve laterally away from the parked car to manage their risk (other interpretations such as managing driving demand results in equivalent controller designs).

Fig.1 shows the testing data for variation of the lateral offset when a risk element is presented within preview, i.e. the parked cars have been detected and the drivers

changed their control behavior according to their sense of security and comfort. The lateral offset tolerance can be derived based on this observed manual vehicle control data variation. For the parked cars avoidance scenarios, the drivers feel the need to slow down the vehicle and steer the vehicle together, so both longitudinal and lateral control need to be considered. Similarly, for the transitions from straight road to the curved road, the drivers also need to conduct such a combined maneuvering actions.

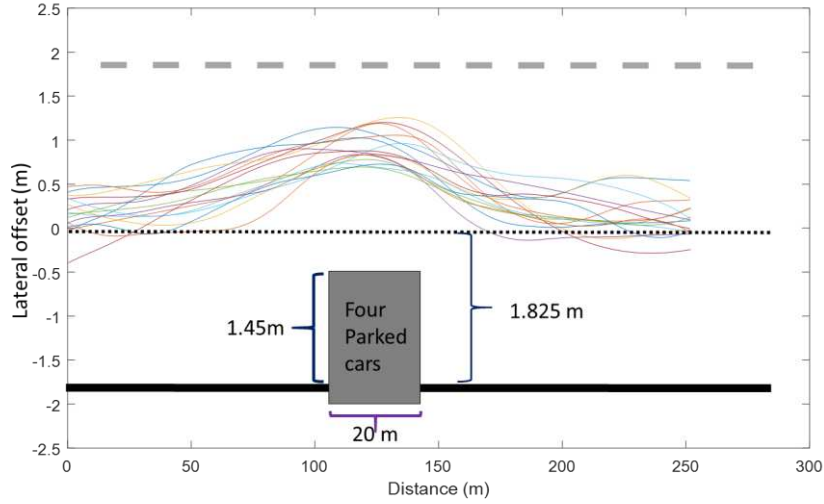


Fig. 1 Lateral offset variation for the parked-cars scenario

3 Models and Results

3.1 Vehicle dynamic model

The vehicle dynamic model used for controller design is simplified to a kinematic bicycle model which is normally used for vehicle motion planning and path tracking as the suspension movement and rolling resistance influences can be neglected.

$$\begin{cases} \dot{y} = -\dot{x}\dot{\psi} + \frac{2}{m}(F_{yf} \cos \delta_f - F_{xf} \sin \delta_f + F_{yr}) \\ \dot{x} = \dot{y}\dot{\psi} + \frac{2}{m}(F_{xf} \cos \delta_f - F_{yf} \sin \delta_f + F_{xr}) \\ \dot{e}_y = \dot{y} + \dot{x}e_\psi \\ \dot{e}_\psi = \dot{\psi} - \dot{x}/R \end{cases} \quad (1)$$

where δ_f is the steer angle of the front wheel, R is the road curve radius in real time. I_z and m represent the vehicle's yaw inertia and mass, respectively. \dot{x} and \dot{y} denote the longitudinal and lateral speeds in the body frame, and $\dot{\psi}$ denotes the yaw rate. F_{yf} , F_{xf} , F_{yr} and F_{xr} represent the lateral and longitudinal tyre forces at the front and rear wheels in coordinate frames aligned with the wheels.

3.2 Tyre model for combined scenario

As for the combined motion scenarios, the longitudinal and lateral force are affected by each other, it is important and necessary to involve this effect into the vehicle model. In this study, we use the Pacejka magic formula tyre model [6] to predict the tyre forces.

At the pure braking or acceleration scenario, the longitudinal force F_{x0} can be expressed by the longitudinal slip ratio λ and the tyre vertical load F_z , which is given by [6]

$$F_{x0} = D_1 \sin\{C_1 \arctan[B_1 \lambda - E_1(B_1 \lambda - \arctan(B_1 \lambda))]\} + S_{Vx} \quad (2)$$

For the pure steering condition, the tyre lateral force F_{y0} can be expressed by tyre slip angle α and tyre vertical load F_z , which is given by [6]

$$\begin{cases} F_{y0} = D_2 \sin\{C_2 \arctan[B_2 \kappa - E_2(B_2 \kappa - \arctan(B_2 \kappa))]\} + S_{Vy} \\ \kappa = \alpha + S_h \end{cases} \quad (3)$$

For the combined steering and braking/acceleration scenarios, the tyre longitudinal force and lateral force are affected by each other. The friction ellipse relationship between the peak longitudinal and lateral tire forces can be assumed, as shown in Figure, for each tyre, the ellipse relationship is given by

$$\left(\frac{F_{x^{**}}}{F_{x0max}}\right)^2 + \left(\frac{F_{y^{**}}}{F_{y0max}}\right)^2 = 1 \quad (4)$$

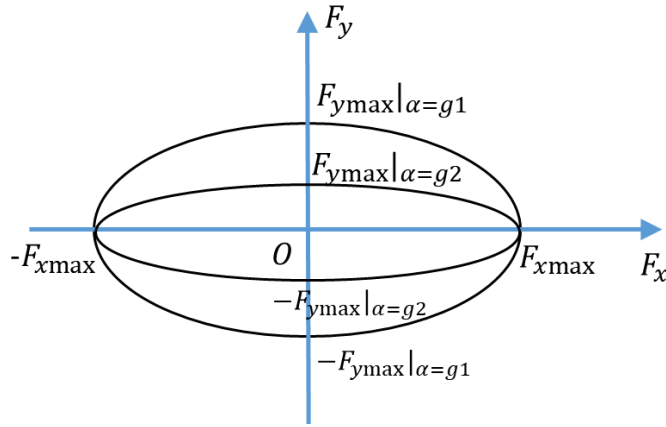


Fig. 2 The tyre lateral and longitudinal relationship at combined scenarios

Therefore, at the combined longitudinal and lateral motion situation, the tyre longitudinal force F_x and lateral force F_y can be expressed by the tyre slip angle α , wheel longitudinal slip ratio λ and tyre vertical load F_z , which is given by

$$F_x = \frac{\sigma_x}{\sigma} F_{x0} \quad (5)$$

$$F_y = \frac{\sigma_y}{\sigma} F_{y0} \quad (6)$$

in which $\sigma = \sqrt{\sigma_x^2 + \sigma_y^2}$, $\sigma_x = -\frac{\lambda}{1+\lambda}$, $\sigma_y = -\frac{\tan \alpha}{1+\lambda}$.

The maximum achievable longitudinal force for the corresponding tire can be obtained by $F_{x0max} = \mu F_z$, and then the tire lateral force F_y for the corresponding tire can be expressed by the tire longitudinal force F_x , which is

$$F_{yi} = P(\kappa) * \sqrt{(\mu F_{zi})^2 - F_{xi}^2} \quad i = f, r \quad (7)$$

where $P(\kappa) = D_2 \sin\{C_2 \arctan[B_2 \kappa - E_2(B_2 \kappa - \arctan(B_2 \kappa))]\} + S_{vy}$. Therefore, the lateral force element F_y in Eq. 1 can be eliminated, which is important for design of the combined motion controller.

3.3 Controller design

To enables the on-board drivers to have a comfortable and natural driving (riding) experience, we set the minimum lateral jerk as the objective in the optimal control. In this study, we developed the Nonlinear Model Predictive Control (NMPC) model with a nonlinear bicycle-type vehicle dynamic model.

Lateral acceleration of the vehicle can be given by

$$a_y = \dot{y} + v_x r \quad (8)$$

While the lateral jerk can be determined by differentiating the lateral acceleration, which is given by

$$j_y = \ddot{y} + \dot{v}_x r + v_x \dot{r} \quad (9)$$

To improve the driving comfort, we define the desired lateral jerk is 0. The lateral offset tolerance (i.e. stay within the corridor that is defined by the manually driver observed data --- or derived from a model capable of producing this corridor; refer to [4]). during the transition is taken as the constraints of the vehicle motion control. Moreover, the vehicle's dynamic constraints including tyre's slip angle, yaw rate, lateral velocity and steering input capability are also considered here.

$$\min_{\Delta U(t)} J(\xi_t, \Delta U(t)) = \sum_{i=1}^{N_p} \|Y_{k+i,t} - Y_{k+i,t}^{ref}\|_Q^2 + \sum_{i=1}^{N_c-1} \|\Delta u_{k+i,t}\|_R^2 + \rho \varepsilon^2 \quad (10)$$

$$\begin{aligned}
s. t. \quad & X_d(k+i+1) = A_d X_d(k+i) + B_d u(k+i), \quad i = 0, 1, \dots, N_p - 1 \\
& Y_d(k+i+1) = C_d X_d(k+i), \quad i = 0, 1, \dots, N_p - 1 \\
& u_{min} \leq u_{k+i,t} \leq u_{max}, \quad i = 0, 1, \dots, N_c - 1 \\
& \Delta u_{min} \leq \Delta u_{k+i,t} \leq \Delta u_{max}, \quad i = 0, 1, \dots, N_c - 1 \\
& Y_{min} - \varepsilon \leq Y_d(k+i+1) \leq Y_{max} + \varepsilon, \quad i = 1, 2, \dots, N_p \\
& Y_{lmin} \leq Y_l(k+i+1) \leq Y_{lmax}, \quad i = 1, 2, \dots, N_p
\end{aligned}$$

where $X_d = [\dot{y}, \dot{x}, \psi, \dot{\psi}, e_y, e_\psi]$ are the needed vehicle states, $Y_d = [\ddot{y}, \ddot{\psi}, \dot{x}, e_y, e_\psi]^T$ are the vehicle output states, $u = [\delta_f, acc]$ is the control inputs. If we express the nonlinear dynamic model of the vehicle system as $\dot{X}_s = f(X_s, u)$, $A_d = \left. \frac{\partial f}{\partial X_s} \right|_{X_s(k), u(k)}$, $B_d = \left. \frac{\partial f}{\partial u} \right|_{X_s(k), u(k)}$, and C_d is the coefficient matrix that used for calculating the outputs. The constraint $Y_{min} - \varepsilon \leq Y_d(k+i+1) \leq Y_{max} + \varepsilon$ represents the limits of vehicle dynamic states in order to guarantee the vehicle's dynamic stability and comfortability. $Y_{lmin} \leq Y_l(k+i+1) \leq Y_{lmax}$ denotes the lateral offset (obtained from observed human driver data).

3.4 Initial results

With the designed controller and the defined road environment, the controller is integrated with our full vehicle model in the driver simulator. Fig.3 shows the comparison between the typical yaw rate profile of a human driver (blue) in the UoLDS and what our controller produces (red). The experimental road contains straight sections, curves, parked cars, etc. . It can be seen that the yaw rate variation has similar magnitude as the driver's yaw rate. Moreover, at the pure curved road and pure straight road, the yaw rate is smoother than the driver's data, which means more comfortability can be obtained under those conditions.

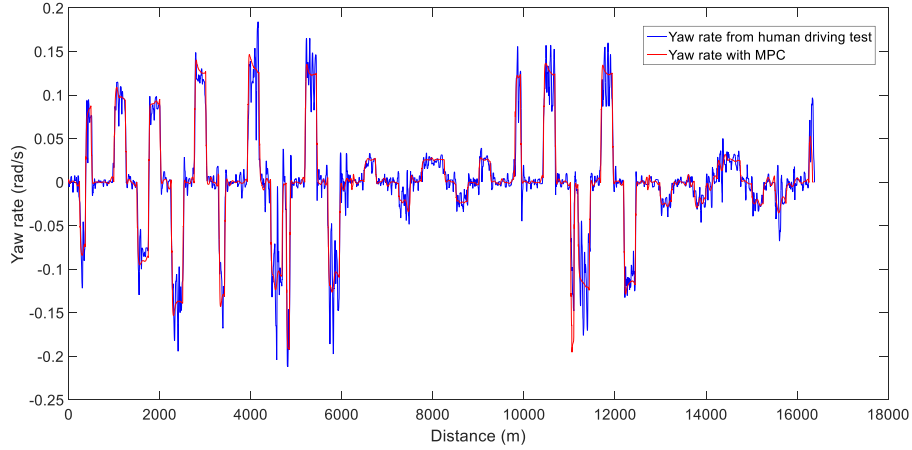


Fig. 3 Predicted yaw rate of the AV at a defined hybrid scenario

4 Conclusions

The goal in this study was to demonstrate that the naturally tolerances that drivers adopt in their driving behavior can be used to develop an autonomous controller that has strikes a balance between obstacle avoidance and smoothness that mimics or supersedes that of human drivers. In this study, we developed a model predictive control model by combining the longitudinal and lateral motions, i.e. steering and braking/acceleration, which is important to be adopted in the obstacle avoidance and straight-to-curve transition scenarios. To improve the driving comfort for the drivers, the controller was designed by optimizing the lateral jerk in the cost function. Results showed that the yaw rate variation along the full road curve is very satisfactory.

Acknowledgement

The work described in this abstract was undertaken in connection with the HumanDrive project which is co-funded by Innovate UK, the UK's innovation agency. This abstract is submitted with kind permission from the HumanDrive consortium: Nissan, Hitachi, Horiba MIRA, Atkins Ltd, Aimsun Ltd, SBD Automotive, University of Leeds, Highways England, Cranfield University and the Connected Places Catapult.

References

- [1] K. Chu, M. Lee and M. Sunwoo, "Local Path Planning for Off-Road Autonomous Driving With Avoidance of Static Obstacles," in *IEEE Transactions on Intelligent Transportation Systems*, vol. 13, no. 4, pp. 1599-1616, Dec. 2012.
- [2] Y. Rasekhipour, A. Khajepour, S. Chen and B. Litkouhi, "A Potential Field-Based Model Predictive Path-Planning Controller for Autonomous Road Vehicles," in *IEEE Transactions on Intelligent Transportation Systems*, vol. 18, no. 5, pp. 1255-1267, May 2017.
- [3] Chongfeng Wei, Richard Romano, Foroogh Hajiseyedjavadi, Natasha Merat, Erwin R. Boer, "Driver-centred Autonomous Vehicle Motion Control within A Blended Corridor", *Advances in Automotive Control - 9th AAC 2019*, In press
- [4] Voß, G.M.I., C.M. Keck, and M. Schwalm, Investigation of drivers' thresholds of a subjectively accepted driving performance with a focus on automated driving. *Transportation Research Part F: Traffic Psychology and Behaviour*, 2018, 56: p. 280-292.
- [5] Boer, E.R., Satisficing Curve Negotiation: Explaining Drivers' Situated Lateral Position Variability. *IFAC-PapersOnLine*, 2016, 49(19): p. 183-188.
- [6] Pacejka HB. Tyre and vehicle dynamics. 2nd ed. *Oxford: Butterworth-Heinemann*; 2005